

In Silico Binding Free Energy Predictability by Using the Linear Interaction Energy (LIE) Method: Bromobenzimidazole CK2 Inhibitors as a Case Study

A. Bortolato and S. Moro*

Molecular Modeling Section, Department of Pharmaceutical Sciences, University of Padova, via Marzolo 5, I-35131 Padova, Italy

Received August 24, 2006

Protein kinase CK2 is essential for cell viability, and its control regards a broad series of cellular events such as gene expression, RNA, and protein synthesis. Evidence of its involvement in tumor development and viral replication indicates CK2 as a potential target of antineoplastic and antiviral drugs. In this study the Linear Interaction Energy (LIE) Method with the Surface Generalized Born (SGB) continuum solvation model was used to study several bromobenzimidazole CK2 inhibitors. This methodology, developed by Åqvist, finds a plausible compromise between accuracy and computational speed in evaluating binding free energy (ΔG_{bind}) values. In this study, two different free binding energy models, named “CK2scoreA” and “CK2scoreB”, were developed using 22 inhibitors as the training set in a stepwise approach useful to appropriately select both the tautomeric form and the starting binding position of each inhibitor. Both models are statistically acceptable. Indeed, the better one is characterized by a correlation coefficient (r^2) of 0.81, and the predictive accuracy was 0.65 kcal/mol. The corresponding validation, using an external test set of 16 analogs, showed a correlation coefficient (q^2) of 0.68 and a prediction root-mean-square error of 0.78 kcal/mol. In this case, the LIE approach has been proved to be an efficient methodology to rationalize the difference of activity, the key interactions, and the different possible binding modes of this specific class of potent CK2 inhibitors.

INTRODUCTION

Phosphoproteome can be defined as the complete set of phosphorylated proteins in a cell. There is a great interest in protein phosphorylation, since it is strictly correlated to protein function and, consequently, to the whole cell life. Protein kinases (PKs) and protein phosphatases exert a tight and reversible control on protein phosphorylation. Both these enzymatic categories can be subdivided into tyrosine- and serine/threonine-specific, based on their catalytic specificity.¹ PKs catalyze the transfer of the γ -phosphoryl group of an ATP or a GTP molecule to the peptide substrate. On the contrary, phosphatases remove the phosphate group from the substrate. In this contest, kinome definitely can be the totality of protein kinases in a cell. Nowadays, thanks to the human genome sequencing, we know almost the total number (518) of human PKs, a large number of genes constituting about 1.7% of all human genome.² Signal transduction, homeostasis, apoptosis, and cell metabolism are some of the many physiological roles controlled by protein kinases. A fine regulation of their activity is essential for the cell life, and a perturbation of this equilibrium is often associated with a number of diseases, including cancer, diabetes, and inflammation.³ As a consequence, this family of enzymes is considered the second most important druggable target of the postgenomic era.⁴

CK2 (casein kinase 2) is one of the first protein kinases discovered.⁵ It is essential for cell viability and with more than 300 peptidic substrates is one of the most known

pleiotropic enzymes.⁶ Its control regards a broad series of cellular events such as cycle regulation, gene expression, and RNA and protein synthesis.⁶ Evidence of CK2 involvement in the regulation of cell polarity and morphology has been recently shown.⁷ CK2 seems to be constitutively active, lacking a strict control commonly present in other kinases.⁶ Its overexpression in a wide variety of tumors,^{8,9} together with the observation that many viruses are exploited in host cell CK2 for the phosphorylation of proteins essential to their life cycle, indicates CK2 as a potential target for antineoplastic and antiviral drugs.¹⁰ Several ATP site-directed CK2 inhibitors have been reported so far, and the structural bases of their potency and selectivity have been clarified by the crystallization of numerous CK2-inhibitor complexes. In particular, 1,8-dihydroxy-4-nitro-xanthen-9-one (MNX), 1,8-dihydroxy-4-nitro-anthraquinone (MNA), and 1,4-diamino-5,8-dihydroxy-anthraquinone (DAA), three similar anthraquinone-related compounds, have shown two different possible binding modes in the CK2 active pocket.¹¹ Other interesting known inhibitors have been already described such as emodin,¹² the indoloquinazoline derivative ([5-oxo-5,6-dihydroindolo-(1,2a)quinazolin-7-yl]acetic acid, IQA),¹³ the tetrabromobenzotriazole (TBB),^{14,15} several flavonoids (like apigenin),^{16,17} benzocoumarins, and coumarins.¹⁸ The available binding modes show several common hydrophobic interactions in the middle of the ATP binding pocket and the presence of hydrogen bonding interactions with the hinge region or with the catalytic aspartate residue (Asp175 in maize CK2). Interestingly, the ATP binding site is smaller than the majority of protein kinases due to the presence of several bulky residues such as Ile 66, Ile 174, and Met 163.

* Corresponding author phone: +39 049 827 5704; fax: +39 049 827 5366; e-mail: stefano.moro@unipd.it.

This peculiarity consents to a small molecule like TBB to selectively inhibit CK2 activity filling with high complementarity the hydrophobic portion of the catalytic cavity. Following this evidence, several new benzimidazole derivatives have been synthesized.^{19,21} Moreover, the structures of K37 (4,5,6,7-tetrabromo-2-(methylsulfanyl)-1H-benzimidazole; PDB code 1ZOG), K44 (N¹,N²-ethylene-2-methylamino-4,5,6,7-tetrabromobenzimidazole; PDB code 1ZOH), and K25 (2-dimethylamino-4,5,6,7-tetrabromo-1H-benzimidazole; PDB code 1ZOE) have been recently cocrystallized with maize CK2, and the corresponding binding motifs have been summarized.²²

The availability of several crystal structures of different TBB-analogues in concert with a large structure–activity relationship (SAR) for this class of CK2 inhibitors suggested to us the possibility to explore the linear interaction energy (LIE) method to build up a binding free energy prediction model of this TBB-like class of CK2 inhibitors. LIE methodology was developed by Åqvist as a plausible compromise between accuracy and computational speed in determining binding free energy (ΔG_{bind}) values.^{23,24} Different authors have already described the applicability and the accuracy of this approach in which free energy predictions have been estimated with an error on the order of 1 kcal/mol.^{25–38} Application of LIE methodology in docking/scoring applications has been also reported.^{39–41} An important key point in using LIE methodology is the accessibility of a reasonable pose of the ligand inside the binding cavity, and, if available, it is usually derived from the crystal structure of the ligand–protein complex. As alternative, a reasonable ligand starting pose, can be obtained by molecular docking simulations, but in this case special attention must be paid to the selection of the most representative binding conformation.^{42,43}

In this study, we have developed a binding free energy prediction model based on all known TBB-like inhibitors by using the LIE method *in tandem* with the Surface Generalized Born (SGB) approximation for the treatment of the electrostatic solvation energy.^{44–46} The CK2-inhibition activity of 45 TBB-like together with the availability of four different crystal structures has been provided as a robust base to build up and evaluate the LIE method performances in both rationalization of the observed binding motifs and in the prediction of the corresponding binding free energies.^{18–20}

MATERIALS AND METHODS

Linear Interaction Energy Method. The LIE method is based on the assumption that the inhibitor free energy of binding to a macromolecule is linearly correlated to several energy terms that can be calculated using a molecular mechanic force field.²³ The ΔG_{bind} is derived using the following formula:

$$\Delta G_{\text{bind}} = \alpha(\langle U_{\text{vdw}}^{\text{b}} \rangle - \langle U_{\text{vdw}}^{\text{f}} \rangle) + \beta(\langle U_{\text{elec}}^{\text{b}} \rangle - \langle U_{\text{elec}}^{\text{f}} \rangle) + \gamma(\langle U_{\text{cav}}^{\text{b}} \rangle - \langle U_{\text{cav}}^{\text{f}} \rangle) \quad (1)$$

Two different simulations must be performed: one describes the molecule free in solution (U^{f}), and the other considers the ligand–protein complex (U^{b}). This is necessary to approximate the binding event as replacement of the interaction of the inhibitor with water molecules, with the interaction

in a mixed aqueous-protein environment. The energy values collected estimate the van der Waals interaction (U_{vdw}), the electrostatic contributions (U_{elec}), and the cavity parameter (U_{cav}). This last one, introduced by Carlson and Jorgensen,⁴⁷ is linked to the energy penalty for forming a solute cavity. Indeed, this term is proportional to the solvent accessible area, and, in addition, it contains a component corresponding to the van der Waals solute–solvent interactions, not zero even for buried atoms up to a certain distance from the solute-exposed surface.⁴⁸ The brackets indicate that the ensemble average of the energy terms is taken into account during the simulation. Using a training set of molecules with known activity, a semiempirical energy model is built by fitting the three different parameter coefficients (α , β , and γ) to the free energy of binding. This empirical element can be useful to compensate part of the limits of the method, due, for example, to the force field or to the difficulty in evaluating the entropic cost in the intramolecular changes of receptors and ligands during the complex formation. In this study the solvent has been treated using the surface-generalized Born (SGB) continuum solvation model, an approach that has been validated in several studies^{38,44–46} and reduces ten times the computational effort. In this method the electrostatic energy is due to a Coulomb (U_{coul}) term and the SGB-solvent reaction energy (U_{rxnf}):

$$U_{\text{elec}} = U_{\text{coul}} + 2U_{\text{rxnf}} \quad (2)$$

Molecular dynamic sampling or Monte Carlo simulation can be used to calculate the energy terms; however, if the initial docked position of the ligands is known, then a simple minimization protocol can provide comparable results with a small degradation of accuracy. A common approach consists of using the crystal structure of an available protein–inhibitor complex as the starting pose for the fast minimization protocol of other molecules with comparable scaffold. The LIE method seems to not permit the parameter transferability³⁸ even if the enzymes belong to the same class; nevertheless, more investigations are needed.

Preparation of CK2. Coordinates of the human CK2 were downloaded from the RSCB Protein Data Bank⁴⁹ (PDB code 1JWH⁵⁰). Only the A chain was used, and the other three monomers were removed together with all water molecules, ions, and the ligand AMP. In the protein were included two water molecules present in the crystal structure of TBB in complex with CK2 and considered important for the binding of inhibitors. TBB (PDB entry 1J91¹⁴) and these two water molecules (Water 1, Water 2) were superimposed to the kinase domain. Using the Protein Preparation⁵¹ utility (Schrödinger Inc.), the residues that were beyond 8–12 Å from TBB were neutralized, possible conflicts in the hydrogen bonding were corrected, and the two alternate tautomers of the histidine side chain were considered, especially if near the binding pocket. Using the OPLS force field the hydrogenated CK2–TBB complex was energy minimized until the average rms deviation of the non-hydrogen atoms reached 0.3 Å. This protocol was exploited for both of the two tautomeric states of TBB, that influences the orientation of the hydrogens of water molecules.

Preparation of Inhibitors. All inhibitors were built using the LigPrep⁵² utility in Maestro (Schrödinger Inc.), and all species existing at pH = 7 ± 1, including tautomers and

Table 1. CK2 Inhibitors Used as a Training Set To Create CK2scoreA and CK2scoreB

inhibitor	R1	R2	R4	R5	R6	R7	K_i (μ M)	ΔG_{exp} (kcal/mol)
1 TBB			-Br	-Br	-Br	-Br	0.60	-8.54
2 diclo-2azaB			-H	-Cl	-Cl	-H	10.00	-6.86
3 tetraclo-2azaB			-Cl	-Cl	-Cl	-Cl	5.00	-7.28
4 K25	-H	-N(CH ₂) ₂	-Br	-Br	-Br	-Br	0.04	-10.16
5 K37	-H	-SCH ₃	-Br	-Br	-Br	-Br	0.07	-9.82
6 DiClBz	-H	-H	-H	-Cl	-Cl	-H	35.00	-6.12
7 TCBz	-H	-H	-Cl	-Cl	-Cl	-Cl	21.00	-6.42
8 TBI	-H	-H	-Br	-Br	-Br	-Br	0.70	-8.45
9	-H	-Br	-Br	-Br	-Br	-Br	0.23	-9.11
10	-H	-NH ₂	-Br	-Br	-Br	-Br	0.09	-9.67
11	-H	-NHCH ₃	-Br	-Br	-Br	-Br	0.09	-9.67
12	-H	-NH(CH ₂) ₂ OH	-Br	-Br	-Br	-Br	0.13	-9.45
13	-H	-NHCH(CH ₃) ₂	-Br	-Br	-Br	-Br	0.06	-9.91
14	-H	-NH(CH ₂) ₂ OCH ₃	-Br	-Br	-Br	-Br	0.14	-9.41
15	-CH ₃	-Br	-Br	-Br	-Br	-Br	0.54	-8.60
16	-CH ₂ CH=CH ₂	-Br	-Br	-Br	-Br	-Br	0.63	-8.51
17	-CH ₃	-OH (=O) ^a	-Br	-Br	-Br	-Br	0.20	-9.20
18	-CH ₃	-N(CH ₃) ₂	-Br	-Br	-Br	-Br	0.20	-9.20
19	-CH ₃	-NHCH(CH ₃) ₂	-Br	-Br	-Br	-Br	0.19	-9.23
20	-CH ₃	-SCH ₃	-Br	-Br	-Br	-Br	0.36	-8.84
21	-H	-SCH ₂ CH(OH)CH ₂ OH	-Br	-Br	-Br	-Br	0.14	-9.41
22	-H	-OH (=O) ^a	-Br	-Br	-Br	-Br	0.15	-9.38
23	-H	-NH(CH ₂) ₂ N(CH ₃) ₂	-Br	-Br	-Br	-Br	0.16	-9.33
24	-CH ₂ CONH ₂	-Br	-Br	-Br	-Br	-Br	1.90	-7.85
25	-H	-SCH ₂ COOH	-Br	-Br	-Br	-Br	0.18	-9.26

^a Both keto- and enol-tautomers were investigated in two different simulations. The keto-tautomer was finally chosen to build both CK2scoreA and CK2scoreB models.

enantiomers, were generated. Using MMFFs force field in vacuum a short conformational search was performed to relax the structure. As a starting pose of the LIE calculation the molecules were superimposed to TBB, K37A, or K37B; since all these ligands have a similar scaffold, it is likely that they share a common binding mode. For every inhibitor the choice of its initial position, enantiomer, or ionic form was made to agree with the chemical-physical considerations on the LIE simulation final pose and with the statistical validation of the LIE final model.

LIE Calculation. The LIE energy model was created using the Liaison package⁵¹ implemented by Schrödinger, Inc. All the calculations were carried out using the OPLS2003 force field, and the implicit solvent was treated using the surface generalized Born (SGB) model. A truncated Newton minimization was performed for free ligands with a residue-based cutoff distance of 15 Å, a 0.01 root-mean-square (rms) gradient for convergence, and a maximum of 500 steps. For the complex CK2-inhibitor has been used the same protocol, but with a rms gradient for convergence of 0.05, and all the protein residue beyond 10 Å from TBB has been frozen. The energy terms calculated with this protocol were used to build the binding free energy models.

Quantum Mechanic Calculations. For molecule **19** present in our training set (Table 1) and for molecule **41** present in the corresponding test set (Table 4) a comparative

semiempirical conformational analysis was performed. Using the force field MMFF94x, a stochastic conformational search in vacuum was carried out with the MOE package⁵³ to detect starting conformations near the energy minimum. From these initial geometries, we have calculated the heat of formation (ΔH_f) of the equilibrium geometry at ground state with the Spartan program.⁵⁴ The semiempirical calculations have been performed with AM1 and PM3 with the aqueous solvation energy using the SM 5.4 procedure of Cramer, Truhlar, and co-workers.⁵⁵

RESULTS AND DISCUSSION

CK2 Crystal Structure. The crystal structures of the *Zea mays* CK2 in complex with tetrabromobenzodiazole derivatives were solved for TBB¹⁴ (PDB code 1J91), K25 (PDB code 1ZOE), K44 (PDB code 1ZOH), and K37 (PDB code 1ZOG).²² The last one presents two different ligand poses called K37A and K37B (as shown in Figure 1). The inhibitor activity assays have been performed using rat CK2 that shares a perfectly identical kinase domain with the human one and presents an identity of 76.1% with *Zea mays* CK2. Indeed, in a range of 6 Å (using TBB as a reference ligand) of the ATP-binding site, only four amino acids are not identical between human and maize CK2: Leu45Val and Val66Ile (positioned on the P-loop), Ile95Val, and His115Tyr (located in the hinge region). However, only the Val66Ile position is

Table 2. Comparison of the Ensemble Average LIE Energy Terms for the Surface Generalized Born Continuum Solvent Model for the Training Set Free State (f) and Bound State (b) between CK2scoreA and CK2scoreB^a

inhibitor		U_{coul}^f (kcal/mol)	U_{vdw}^f (kcal/mol)	U_{rxnf}^f (kcal/mol)	U_{cav}^f (kcal/mol)	U_{coul}^b (kcal/mol)	U_{vdw}^b (kcal/mol)	U_{rxnf}^b (kcal/mol)	U_{cav}^b (kcal/mol)
1	CK2scoreA	0	0	-7.3369	-3.9708	-25.9540	-28.2600	-1.1124	-1.6834
	CK2scoreB	0	0	-7.3369	-3.9708	-25.9540	-28.2600	-1.1124	-1.6834
2	CK2scoreA	0	0	-8.0632	-1.9537	-26.5010	-18.6490	-0.5601	-0.3302
	CK2scoreB	0	0	-8.0632	-1.9537	-26.5010	-18.6490	-0.5601	-0.3302
3	CK2scoreA	0	0	-8.2269	-2.6004	-20.3440	-25.7910	-1.5122	-0.1051
	CK2scoreB	0	0	-8.2269	-2.6004	-20.3440	-25.7910	-1.5122	-0.1051
4	CK2scoreA	0	0	-7.8606	-4.5924	-8.8304	-36.4620	-3.6214	0.0487
	CK2scoreB	0	0	-7.8606	-4.5924	-8.8304	-36.4620	-3.6214	0.0487
5	CK2scoreA	0	0	-5.8040	-3.2395	0.6488	-39.5260	-3.8976	0.0560
	CK2scoreB	0	0	-8.2309	-3.5706	-5.4229	-37.4250	-5.5969	0.0276
6	CK2scoreA	0	0	-10.6060	-1.1149	-27.1810	-17.3850	-1.9863	0.2891
	CK2scoreB	0	0	-10.6060	-1.1149	-27.1810	-17.3850	-1.9863	0.2891
7	CK2scoreA	0	0	-9.9687	-1.8555	-27.0050	-23.9830	-2.3543	-0.1418
	CK2scoreB	0	0	-9.9687	-1.8555	-27.0050	-23.9830	-2.3543	-0.1418
8	CK2scoreA	0	0	-7.6129	-3.0885	-24.4980	-27.5350	-1.6406	-0.1457
	CK2scoreB	0	0	-7.6129	-3.0885	-24.4980	-27.5350	-1.6406	-0.1457
9	CK2scoreA	0	0	-6.0590	-3.8315	-1.3455	-38.3150	-4.0858	-0.6597
	CK2scoreB	0	0	-6.1283	-4.1155	-1.8397	-37.0610	-3.3133	-0.4056
10	CK2scoreA	0	0	-11.0160	-4.9734	0.0713	-36.2320	-6.5187	-6.5187
	CK2scoreB	0	0	-11.1650	-5.0441	-14.3230	-33.1000	-6.3554	-1.2314
11	CK2scoreA	0	0	-8.4315	-5.2075	0.7733	-37.7250	-5.2796	-0.9014
	CK2scoreB	0	0	-8.7779	-5.2547	-12.2000	-34.1390	-4.1418	-0.2877
12	CK2scoreA	0	0	-13.6680	-5.1610	-12.2250	-37.5540	-7.3914	-0.9671
	CK2scoreB	0	0	-13.6070	-5.1384	-16.6110	-37.1250	-5.9417	-0.1172
13	CK2scoreA	0	0	-7.7826	-5.0738	0.2795	-40.2860	-4.9879	-0.6444
	CK2scoreB	0	0	-7.8203	-5.0567	-11.9860	-37.8760	-3.4786	0.3434
14	CK2scoreA	0	0	-9.6616	-5.3114	-0.0291	-40.6240	-5.3420	-0.6836
	CK2scoreB	0	0	-9.4952	-5.3267	-15.2920	-39.2910	-4.1977	0.1101
15	CK2scoreA	0	0	-2.6495	-2.2237	-1.2393	-39.8380	-1.8082	0.0983
	CK2scoreB	0	0	-2.8130	-2.5318	-2.3673	-38.0970	-1.6814	0.3324
16	CK2scoreA	0	0	-2.6057	-2.0137	-1.9885	-42.2550	-1.8014	2.6127
	CK2scoreB	0	0	-3.0168	-2.3688	-3.8413	-40.8160	-1.6899	0.6311
17	CK2scoreA	0	0	-10.3210	-6.0790	-6.1568	-36.6910	-4.7716	-1.2720
	CK2scoreB	0	0	-10.9300	-6.1630	-12.9160	-33.890	-4.7848	-1.0334
18	CK2scoreA	0	0	-4.5568	-3.2973	0.2302	-41.5190	-2.7188	0.8368
	CK2scoreB	0	0	-4.5959	-3.1823	-7.2072	-39.3360	-2.4997	1.1179
19	CK2scoreA	0	0	-4.7107	-3.5682	-1.1517	-40.8110	-3.4040	0.0289
	CK2scoreB	0	0	-5.1187	-3.6615	-13.6370	-38.6240	-2.337	0.9863
20	CK2scoreA	0	0	-4.2830	-1.8848	-1.5686	-41.3510	-2.9071	0.6429
	CK2scoreB	0	0	-4.7006	-2.2029	-7.4554	-39.8620	-2.1566	0.8545
21	CK2scoreA	0	0	-19.9740	-3.5731	-29.9950	-38.1490	-13.4830	-6.9798
	CK2scoreB	0	0	-21.0080	-3.8815	-41.3180	-38.9110	-6.4401	-0.5889
22	CK2scoreA	0	0	-11.5860	-6.6001	-5.4465	-36.0510	-5.1827	-1.5775
	CK2scoreB	0	0	-12.1450	-6.9093	-27.1050	-31.8910	-1.8854	-0.3021
23	CK2scoreA	0	0	-73.5960	-3.5507	54.8200	-42.1260	-3.7417	0.2921
	CK2scoreB	0	0	-74.3630	-3.3062	38.8130	-41.9110	-39.8020	-0.3901
24	CK2scoreA	0	0	-8.6384	-5.1098	-24.1580	-34.1820	-3.6828	-0.4103
	CK2scoreB	0	0	-8.9871	-5.3484	-8.9025	-41.0740	-4.5262	0.1529
25	CK2scoreA	0	0	-76.8190	-4.2250	-117.1700	-36.8700	-68.7050	-0.6296
	CK2scoreB	0	0	-77.3850	-4.5163	-122.9700	-40.4070	-47.5200	-0.1659

^a U_{coul} , U_{vdw} , U_{rxnf} , and U_{cav} are the Coulomb, van der Waals, Reaction Field, and Cavity energy terms. ^b The absence of explicit interaction between the ligands and solvent in the free state results in a van der Waals and Coulomb energy equal to zero.

closed to the ligand-binding region. Following this structure similarity, in this computational study we selected the crystal of human CK2 in complex with an ATP analogue (PDB entry 1JWH)⁵⁰ as the reference structure. Another important issue considered in the present study was the induced fit by the ligand to the residue His160; according to the available crystal structures His160 can assume two different conformers depending on the nature of the inhibitor bound. According to the B-factors, both conformers should be plausible. In the present study, we have approximated two distinct binding modes: the first one similar to TBB (TBB-like binding mode) with histidine in a “close” position and a second one (K-like binding mode) with histidine in an “open” conformation. In particular, the crystal structures of the maize CK2,

His160 is its open-status leaving the active site completely accessible to K-like analogues.

Water Molecules and Inhibitor Binding Modes. Pospisil et al. have recently demonstrated the critical role of explicit water molecules in structure-based drug design applications.⁵⁶ In this LIE study, we decided to include two water molecules in the active site of the human CK2, derived from the crystal structure of the protein in complex with TBB (Water 1 and Water 2, PDB code 1J91).¹⁴ Water 2 is structurally conserved in all available crystal structures, while Water 1 can be replaced by ions such as chloride (K25; PDB code: 1ZOE) or sodium (K44; PDB code: 1ZOH). Theoretically, each TBB-like inhibitor might have the possibility of interacting through hydrogen bonding with Water 1 (Figure 1). More-

Table 3. Comparison of Experimental (ΔG_{exp} , kcal/mol), Predicted ($\Delta G_{\text{CK2scoreA}}$ and $\Delta G_{\text{CK2scoreB}}$, kcal/mol), and Jackknife Cross-Validated (ΔG_{CV_A} and ΔG_{CV_B} , kcal/mol) Free Energies of Binding between the Two Energy Models CK2scoreA and CK2scoreB for the Training Set

inhibitor	ΔG_{exp} (kcal/mol)	$\Delta G_{\text{CK2scoreA}}$ (kcal/mol)	ΔG_{CV_A} (kcal/mol)	$\Delta G_{\text{CK2scoreB}}$ (kcal/mol)	ΔG_{CV_B} (kcal/mol)
1	-8.54	-8.93	-9.07	-8.61	-8.62
2	-6.86	-5.93	-5.79	-5.85	-5.70
3	-7.28	-6.96	-6.94	-6.82	-6.80
4	-10.16	-9.93	-9.90	-9.14	-9.04
5	-9.82	-9.03	-8.95	-8.83	-8.71
6	-6.12	-4.91	-4.80	-5.04	-4.90
7	-6.42	-6.44	-6.44	-6.64	-6.69
8	-8.45	-8.07	-8.00	-7.97	-7.89
9	-9.11	-8.68	-8.65	-8.38	-8.23
10	-9.67	-7.99	-7.76	-8.59	-8.52
11	-9.67	-9.29	-9.24	-9.12	-9.07
12	-9.45	-9.72	-9.74	-9.54	-9.55
13	-9.91	-9.93	-9.93	-10.08	-10.10
14	-9.41	-9.91	-9.99	-10.52	-10.63
15	-8.60	-8.66	-8.68	-8.61	-8.61
16	-8.51	-9.11	-9.31	-9.31	-9.50
17	-9.20	-9.67	-9.75	-8.90	-8.86
18	-9.20	-10.07	-10.14	-9.82	-9.87
19	-9.23	-9.73	-9.77	-10.39	-10.48
20	-8.84	-9.02	-9.06	-9.28	-9.36
21	-9.41	-10.22	-10.52	-10.27	-10.46
22	-9.38	-9.53	-9.57	-9.84	-10.14

over, we have considered all possible tautomeric forms of the imidazole moiety to correctly evaluate which tautomer might preferably bind the water molecule. Interestingly, the minimization protocol applied to the K37B-CK2 complex was able to reproduce the crystallographic pose of Water 1 found in the corresponding crystal structure (H₂O1227; PDB code 1ZOG).²² In this LIE study, for all other inhibitors not yet crystallized in complex with CK2, we have considered three possible starting poses in the minimization protocol: TBB-like, K37A-like, or K37B-like binding mode (Figure 1).

Training Set. As summarized in Table 1, all benzoimidazole derivatives (25 compounds) with a known inhibitory constant (K_i) value were used as a training set to build up a LIE model. From a structural point of view, the main difference among them is the nature of the substituent at position 2. As already anticipated, the possible different starting pose of ligands (TBB-like, K37A-like, or K37B-like), the possible tautomeric forms, and, in some case, the different ionic states have been taken into account during the construction of all LIE models.

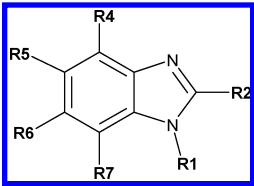
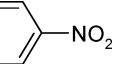
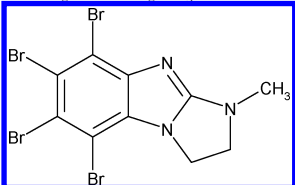
Two different criteria were applied to evaluate which combinations of effects better correlated with experimental K_i values. The first one is based on the quality of the final pose resulting after the minimization protocol. In particular, since the conformational search with this method is extremely limited, it is important that each starting pose is reasonably close to a local energy minimum. An appropriate visual inspection in tandem with a structural and a potential energy analysis have been performed to properly evaluate the quality of each final pose. The second criterion is based on the statistical validation and cross-validation of the LIE energy model. Following the abovementioned strategy, we have developed a stepwise workflow as shown in Figure 2. The first LIE model was created using a small subset of the entire training set characterized by the highest structural similarity

to TBB, K25, and K37. The starting poses for TBB, K25, and K37 were simply collected from the corresponding crystal structures, whereas for all analogues we have used TBB and K37 poses as a template for their structural superimpositions into the CK2 binding cavity. In this way, possible errors due to erroneous starting poses were minimized. After both chemical-physical and the statistical validations, this first model has been progressively implemented with including one by one all the remaining structures until the creation of the final LIE model. Since the crystal structure of the CK2–K37 complex highlights two possible binding modes (A and B) of the K37 inhibitor, we investigated and compared both starting poses as possible templates for the superimposition of all other TBB-like derivatives. Consequently, two different energy models were ultimately obtained: “CK2scoreA” created by using as starting poses those from TBB and K37A and “CK2scoreB” based on TBB and K37B conformations. This stepwise protocol is very useful to create simple “binding mode rules” able to generate robust binding free energy models and helpful to understand which chemical features can relevantly determine the final binding pose (Figure 3). For example, using this approach, we were able to select the carbonyl form instead of the corresponding enol-tautomer for both **17** and **22** derivatives comparing the quality of the corresponding pK_i prediction with respect to the experimental data (see Table 3). Analogously, we found that K25 is probably unprotonated in its bounded state, on the contrary of what Pagano et al. previously suggested.¹⁹

The calculated energy terms, collected in Table 2, underline that the most crucial binding interactions in this TBB-like class of inhibitors are due to hydrophobic and van der Waals contributions and, in particular, emphasize the importance played by the solvent accessible area, which is linked to the energy penalty for forming a solute cavity (U_{cav}). Moreover, the analysis of the binding energy terms indicate that the presence of a polybromide moiety guarantees the necessary driving force for the ligand binding into the CK2 active site. An additional hydrogen bonding with water (Water 1), or further van der Waals interactions of the substituent at position 2, provides the final binding mode of each ligands.

Both CK2scoreA and CK2scoreB models indicate molecules **23**, **24**, and **25** as possible outliers. In fact, the predicted energy values are considerably different from the experimental data. A possible explanation might be found considering some chemical peculiarities of these three TBB-like derivatives. Considering the CK2scoreB model, ligand **23** contains a protonable tertiary amine in the side chain at the 2-position that, apparently, does not interact with any CK2 residues in the bound state. Therefore, the equilibrium is moved to the direction of the free molecule in solution rather than the bound state, and an evaluation with CK2score gives a subestimated free energy of about 10 kcal/mol. Considering derivative **25** in its K37B-like pose, the carboxyl group interacts so strongly with the hydroxyl moiety of Ser51, located in the P-loop domain, that the LIE model overestimated the free binding energy of 7 kcal/mol. The well-known mobility of this region of the protein kinase does not allow us to consistently speculate on this tight interaction, even if in principle it is achievable. The modeling study of inhibitor **24** presents the same type of misinterpretation as

Table 4. CK2 Inhibitors Used as Test Set for Both CK2scoreA and CK2scoreB Models

inhibitor	R1	R2	R4	R5	R6	R7	IC ₅₀ (μ M)	ΔG_{exp} (kcal/mol)
								
26	-H	-CF ₃	-H	-Br	-Br	-H	28.00	-6.25
27	-H	-CF ₃	-Br	-H	-Br	-H	40.00	-6.04
28	-H	-CF ₃	-Br	-Br	-Br	-H	1.20	-8.13
29	-H	-CF ₃	-Br	-Br	-Br	-Br	0.60	-8.54
30	-CH ₃	-CF ₃	-Br	-Br	-Br	-Br	1.71	-7.92
31	-CH ₂ CH ₃	-CF ₃	-Br	-Br	-Br	-Br	6.12	-7.16
32	-H	-CF ₂ CF ₃	-Br	-Br	-Br	-Br	0.40	-8.78
33	-H	-(CF ₂) ₂ CF ₃	-Br	-Br	-Br	-Br	1.28	-8.09
34	-H	-(CF ₂) ₃ CF ₃	-Br	-Br	-Br	-Br	1.48	-8.00
35	-H	-Cl	-Br	-Br	-Br	-Br	0.49	-8.66
36	-H	-CF ₃	-Br	-Cl	-Br	-Br	0.39	-8.80
37	-H	-CF ₃	-Cl	-Br	-Cl	-Br	1.25	-8.10
38	-H	-CF ₃	-Br	-Cl	-Cl	-Br	1.96	-7.83
39	-H	-SH	-Br	-Br	-Br	-Br	0.91	-8.29
40	-H	-CF ₃	-H	-H	-Br	-H	40.00	-6.04
41	-CH ₃	-OCH(CH ₃) ₂	-Br	-Br	-Br	-Br	20.39	-6.44
42	-CH ₃	-OCH ₂ CH ₃	-Br	-Br	-Br	-Br	40.00	-6.04
43	-H	-S- 	-Br	-Br	-Br	-Br	3.48	-7.49
44	-H	-SCH ₂ COOCH ₂ CH ₃	-Br	-Br	-Br	-Br	1.55	-7.97
45 K44							0.10 ^a	-9.61

^a K_i was used instead of IC₅₀.

argued for **25**: in this case, the amide group in the side chain at the 2-position can strongly interact with the backbone of His160. As already anticipated, the conformational mobility of this specific residue, again, does not allow us to appropriately quantify this interaction overestimating the corresponding binding free energy of about 2.5 kcal/mol. Similarly, also the CK2scoreA model overestimates both **24** and **25** inhibitors due to the orientation of the side chain at the 2-position toward a region of the binding cavity more exposed to the solvent and consequently less easier to precisely quantify the solvation energy term of these poses. For these reasons, we have considered molecules **23**, **24**, and **25** as outliers, and, consequently, they were not included in the training set used to build up the final energy models. Moreover, also K44 has not been included in the training set but incorporated in the test set, because its binding mode is more rotated toward the hinge region (Figure 1) with respect to all other TBB-like inhibitors.

Both final LIE energy models, CK2scoreA and CK2scoreB, show acceptable statistics even if the CK2scoreA model presents a slightly better performance, as summarized in Chart 1. Moreover, in Table 3 are collected the experimental and the predicted binding free energies (ΔG_{bind}) for both models. CK2scoreA energy terms resulted in the following: $\alpha = 0.173 \pm 0.003$, $\beta = 0.081 \pm 0.005$, and $\gamma = -0.772 \pm 0.027$. It is very clear that, for this class of CK2 inhibitors,

the energy penalty coming from the formation of a solute cavity (γ coefficient) seems to play a crucial role in determining ligand binding. Probably this is one of the most important driving forces in determining the ligand movement from outside to the binding cavity, where the stabilizing van der Waals interactions are suddenly established (α coefficient). The complementary between the tetrabromobenzo moiety and the protein active site is almost perfect, and its importance is highlighted by the significant loss of activity caused by the substitution of one of these bromides with chloride atoms. The final minimized posed shows that, in several molecules, the substituent in 2 can contribute with additional van der Waals interactions. Similar consideration can be made for CK2scoreB, where energy terms resulted to be the following: $\alpha = 0.191 \pm 0.003$, $\beta = 0.108 \pm 0.007$, and $\gamma = -0.460 \pm 0.025$. In this second model the cavity contribution is still the crucial contributor to binding free energy even if less than for CK2scoreA. This result is in agreement with the consideration that electrostatic interactions with Water 1 or with Asp175 are not accessible for the K37A-like binding mode, while are often established in the K37B-like. Moreover, CK2score energy terms analysis is also compatible with the alogen-driven binding hypothesis proposed by Battistutta et al.²²

Test Set. CK2score was validated with an external test set of 20 inhibitors with known IC₅₀ (Table 4). In this case

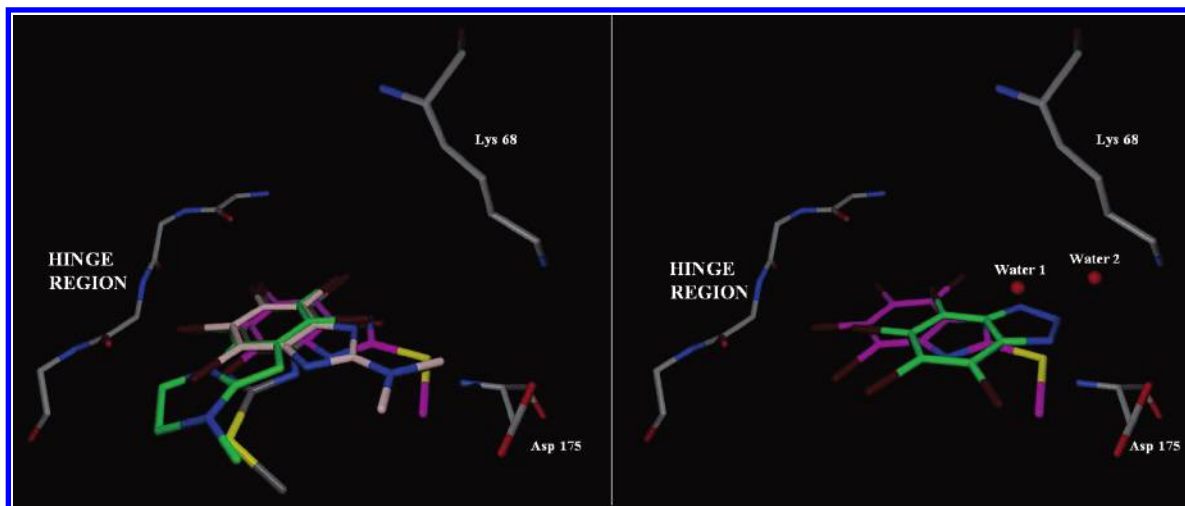


Figure 1. CK2 ATP binding site from an X-ray diffraction crystal structure (PDB entry 1JWH).⁴⁸ The residue Lys68 and the catalytic amino acid Asp175 are shown, together with the Hinge region (the side chains are hidden). *On the left*, the superimposition of K25 (white, PDB entry 1ZOE), K44 (green, PDB entry 1ZOH), and K37 A and B (respectively gray and magenta, PDB entry 1ZOG)²² point out that the hydrophobic interactions are almost the same. The molecules rotate around the benzo moiety, and three out of the four bromides are in a conserved position. *On the right*, TBB (green, PDB entry 1J91)¹⁴ is superimposed to K37 in conformation B (magenta, PDB entry 1ZOG).²² For this computational study CK2 from the PDB 1JWH⁴⁸ was used with the two water molecules from PDB 1J91¹⁴ (shown on the right). While the second water molecule (Water 2) is preserved in all of these crystals, the first one (Water 1) can be substituted by a chloride or sodium ion, and its location can change in a way that seems directly correlated to the structure and final inhibitor pose. For the energy model CK2scoreA the starting LIE position of each inhibitor, without the crystal structure available, was obtained by analogy to TBB and K37A, whereas CK2scoreB was built on the binding mode of TBB and K37B.

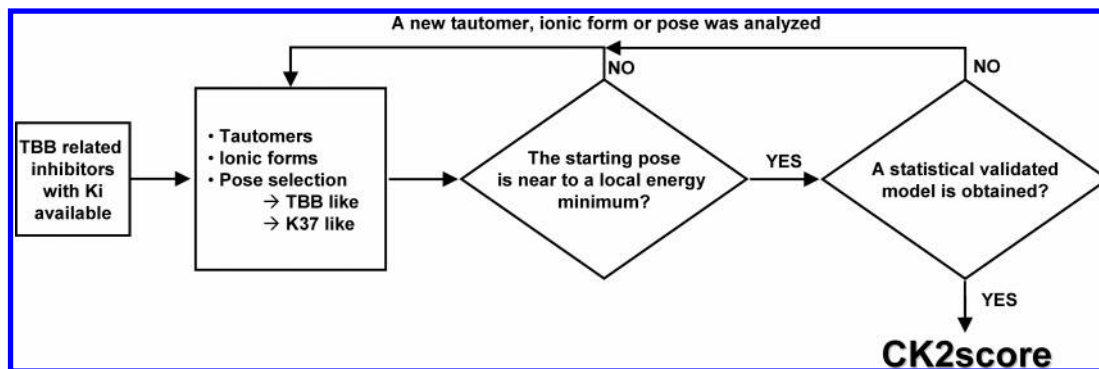


Figure 2. Workflow used to select the inhibitor starting pose and tautomeric and ionic form. An initial model was built using a small set of molecules composed by ligands crystallized in a complex with CK2 and their most structurally related compounds. Starting from the more reasonable pose, tautomeric forms, and ionic state hypothesis, a first model was built. Its validation was both chemical-physical, checking if the energy minimization protocol was found near a local energy minimum and a plausible pose (in a way similar to the docking visual inspection), and statistical, using the correlation factor and cross-validated q^2 . After that the model was progressively implemented with the remaining molecules, with special attention to their tautomeric and ionic hypothesis, their starting and final pose, and the energy terms calculated during the minimization (van der Waals, Electrostatic, Reaction Field, and Cavity energy terms). With this approach if some inhibitors were not linearly correlated to the others, they were considered outlier and excluded from the final model, denominated CK2score. This deep molecular interaction study is useful to try to understand the meaning of these outliers.

we have used IC_{50} instead of K_i considering that it has been precedently demonstrated the correlation between IC_{50} and K_i in the CK2 inhibitory activity assay.¹⁹ For all test set inhibitors, starting binding poses and tautomeric forms have been chosen following the same criteria developed and validated during the LIE model generation.

From a statistical point of view, the predictability of the CK2scoreA model is significantly better than CK2scoreB ($q^2 = 0.676$ and $q^2 = 0.457$, respectively) as summarized in Chart 2. This might be interpreted as a preference for all inhibitors considered in the test set to preferentially adopt a K37A-like binding pose. Moreover, we have identified four possible outliers (41, 42, 43, and 44) in generating the CK2scoreA model and only three outliers (42, 43, and 44) in generating the CK2scoreB model.

Interestingly both the energy models identified three commons outliers (43, 44, and 42) indicating that this specific behavior is pose-independent. Moreover, the fourth outlier (derivative 41) was specifically identified by the CK2scoreA model. Derivative 43, overestimated by about 2.5 kcal/mol by both models, contains a nitrobenzo substituent at the 2-position not present in any ligands used in the training set. In the final poses, this side chain creates several favorable van der Waals interactions, that result in an overestimation of its binding affinity. This overestimation can be explained considering the loss of rotational degrees of freedom during the complex formation resulting in an important reduction of entropy. This relevant entropic factor is probably diluted into the different energy terms of the LIE model parameters altering the prediction of its real binding free energy. For

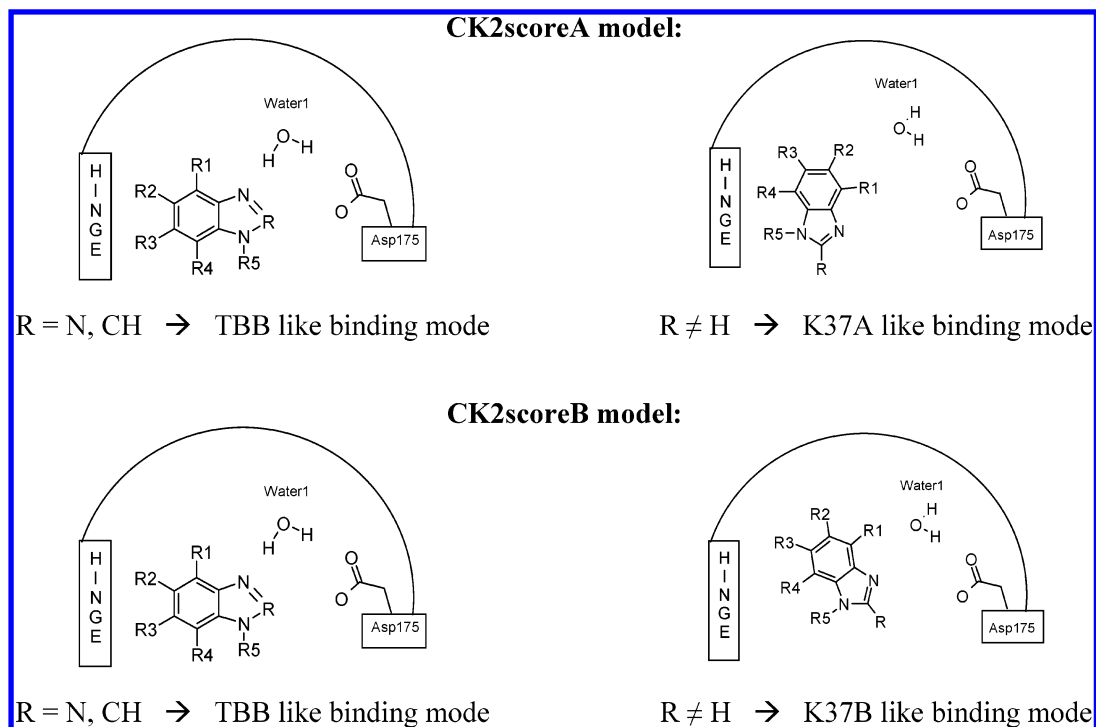
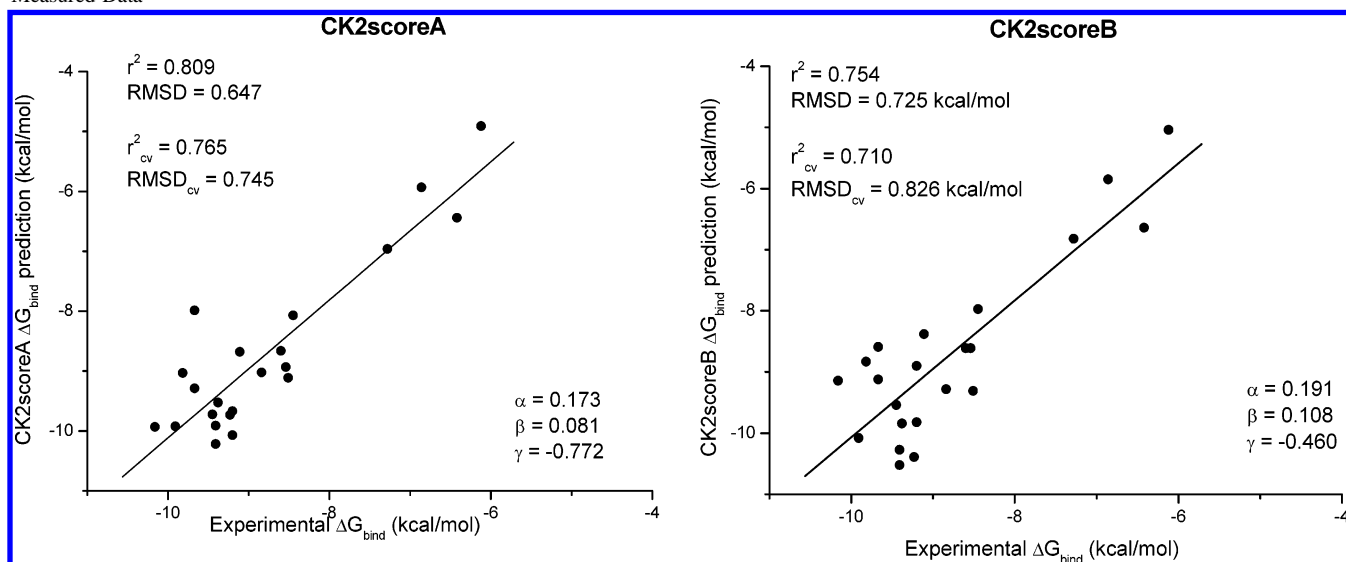


Figure 3. Binding modes rules derived from the best models CK2scoreA and CK2scoreB. The starting pose was chosen according to the moiety in position 2. Both the tautomeric forms were investigated during the model creation. The final choice shown is the one resulting in the energy model with the best r^2 and r^2_{cv} . For CK2scoreA the possible binding modes are TBB-like and K37A-like, while for CK2scoreB they are TBB-like and K37B-like.

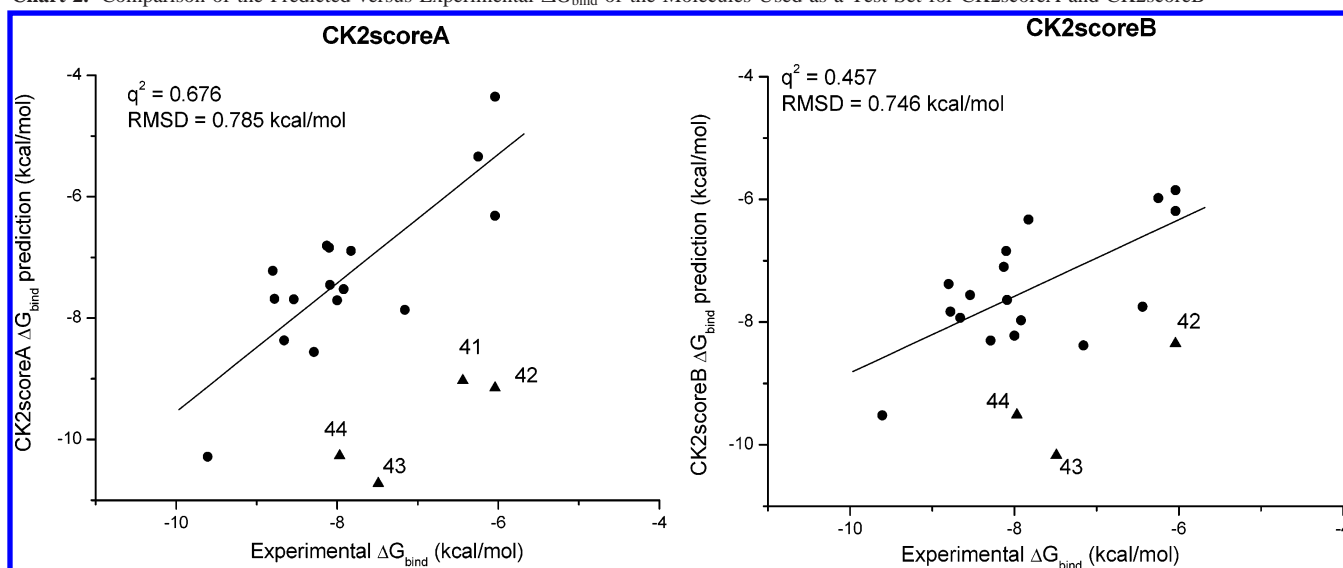
Chart 1. Free Energy of Binding Estimated by CK2scoreA and CK2scoreB of Each Inhibitor Used in the Training Set versus the Experimentally Measured Data^a



^a Correlation coefficient (r^2) and cross-validated coefficient (r^2_{cv}) are shown. For the whole set rmsd and cross-validate rmsd (rmsd_{cv}) were calculated. α , β , and γ are the resulting coefficients of the LIE equation for CK2score.

the second outlier (derivative **44**) in its K37B-like binding mode, a stabilizing hydrogen bonding interaction is formed between the ester moiety of the side chain at the 2-position and the exposed hydroxyl group of Ser51. We already described a very similar phenomena considering derivative **25** of the training set. Nevertheless, in this case CK2scoreB overestimates only about 2.5 kcal/mol instead of the 7 kcal/mol of molecule **25**. This is in agreement with the weaker interaction formed by the ester group with respect to the one formed by the carboxyl moiety of inhibitor **25**. Moreover, we have used the CK2scoreB model to understand what determines a 2-fold difference of activity transforming the

amino group present in **19** in an oxygen as present in molecule **41**. A quantum-mechanic conformational analysis with the aqueous solvation energy⁵⁴ points out that the amino moiety provides two different conformations corresponding to comparable energy minimums. The first conformer, in the final energy minimized docked position, creates two hydrogen bonds: the first with the water molecule (Water 1) and the second with the catalytic aspartic acid Asp175 (Figure 4A). Whereas in the second conformer, the amino group is rotated about 180 degrees, and the steric hindrance of the isopropyl moiety does not allow any hydrogen bonding interactions (Figure 4B). On the contrary, for molecule **41**

Chart 2. Comparison of the Predicted versus Experimental ΔG_{bind} of the Molecules Used as a Test Set for CK2scoreA and CK2scoreB^a

^a RMSD and q^2 are referred to as linear fit of the points indicated with circles. The points represented by triangles are outliers, and their number is referred to in Table 4.

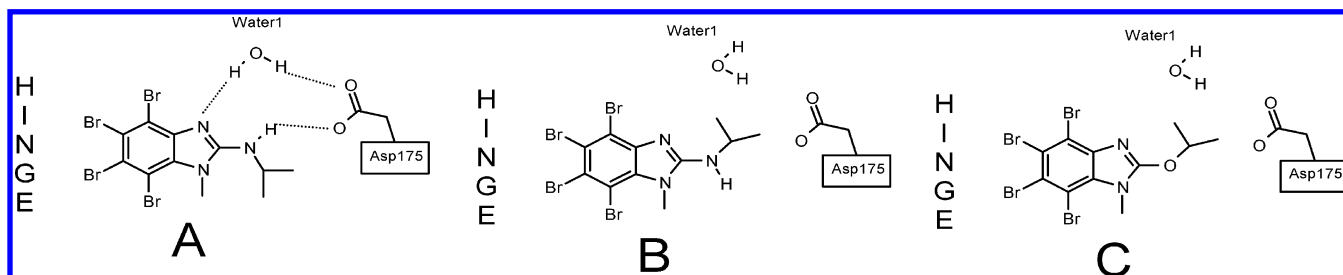


Figure 4. Comparison between the possible binding mode of molecule **19** of the training set ($K_i = 0.19 \mu\text{M}$) and molecule **41** of the test set ($\text{IC}_{50} = 20.39 \mu\text{M}$). Quantum mechanical study with the aqueous solvation energy⁵³ of ligand **19** points out two different absolute energy minimum conformations. (A) In the first one, finally used for the LIE study, the inhibitor creates two instances of hydrogen bonding, one with a Water 1 and the other with the catalytic aspartic acid. (B) In the second one, there is no electrostatic interaction with the protein. (C) For molecule **41**, the only energy minimum present corresponds to this last one of ligand **19**, and no hydrogen bonding is created with CK2.

Table 5. Observed (ΔG_{exp} , kcal/mol) and Calculated ($\Delta G_{\text{CK2scoreA}}$ and $\Delta G_{\text{CK2scoreB}}$, kcal/mol) Free Energies of Binding Obtained for the Test Set by CK2scoreA and CK2scoreB Models

inhibitor	ΔG_{exp} (kcal/mol)	$\Delta G_{\text{CK2scoreA}}$ (kcal/mol)	$\Delta G_{\text{CK2scoreB}}$ (kcal/mol)
26	-6.25	-5.34	-5.98
27	-6.04	-6.31	-6.19
28	-8.13	-6.81	-7.10
29	-8.54	-7.69	-7.56
30	-7.92	-7.52	-7.97
31	-7.16	-7.86	-8.38
32	-8.78	-7.68	-7.83
33	-8.09	-7.45	-7.64
34	-8.00	-7.71	-8.22
35	-8.66	-8.38	-7.93
36	-8.80	-7.22	-7.38
37	-8.10	-6.84	-6.84
38	-7.83	-6.89	-6.33
39	-8.29	-8.56	-8.30
40	-6.04	-4.35	-5.85
41	-6.44	-9.03	-7.75
42	-6.04	-9.15	-8.35
43	-7.49	-10.72	-10.17
44	-7.97	-10.27	-9.51
45	-9.61	-10.28	-9.52

only this last conformer exists, owing to the repulsion of the oxygen and imidazole nitrogen lone pairs (Figure 4C). Through the semiempiric AM1 calculation, the rotational

isomer of molecule **41**, corresponding to the other minimum of molecule **19** of the training set, is estimated to have an energy of 8.9 kcal/mol higher than the absolute minimum. The conformational analysis of derivative **42** provides similar results to derivative **41**. However, using the correct starting poses resulting from the quantum-mechanical conformational study, CK2score overestimates molecule **41** and **42**. Concluding, the missing of entropic contributions, erroneous estimations of the inhibitor internal energy resulting from the binding conformation, and dynamic interactions with different conformational states of the protein are only some of the possible limits of the LIE approach in predicting binding free energies.

Another interesting consideration can be made considering the capacity of the CK2scoreB model to accurately predict the energy of binding of K44, characterized by a binding mode of the bromobenzoimidazole scaffold rotated around the benzo moiety toward the hinge region, a position similar to K37A. This observation can be useful in understanding the differences and the robustness of the two alternative LIE models.

CONCLUSIONS

The proposed stepwise protocol in combination with the linear interaction method provides a powerful and fast

computational technique to accurately predict the binding free energies of this potent class of CK2 inhibitors. The estimated energy terms (α , β , and γ), the calculated interaction energies, the starting binding poses, and the corresponding final minimized poses, together with a robust statistical validation, can be utilized to appropriately describe at the molecular level the possible differences in the CK2-inhibitor recognition processes. In this scenario, the presence of outliers can be useful in understanding the limits of the model and the applicability of the theoretical framework. Moreover, it also offers a chemical insight into the key binding interactions, such as the possible role of water molecules, and rationalizes the different binding modes shown by the available crystal structures. This important knowledge can be the key for a possible development of new bromobenzimidazole derivatives. For example, it could be interesting to understand if all four bromide moieties are equally important for the ligand binding or if one of these could be substituted to obtain hydrogen bonding with the hinge region. To achieve a dual polar interaction at the two opposite sites of the ATP-binding pocket was in fact demonstrated by the new inhibitor ellagic acid to improve greatly the inhibitor activity.⁵⁷

We are currently investigating the possibility to implement our CK2score model with others different scaffolds from known CK2 inhibitors. Different inhibitors binding modes could be investigated accurately using the LIE approach shown in this work. Even if crystal structures of their complex with the protein are not available, the starting poses used for the LIE study can be obtained using common docking programs. The purpose could be to try to map the key parts of the ligands and how they can effect binding modes or the coefficients of the LIE equation.

ACKNOWLEDGMENT

The molecular modeling work coordinated by S.M. has been carried out with financial support from the Italian Ministry for University and Research (MIUR), Rome, Italy and from the University of Padova, Padova, Italy. S.M. is very grateful to Stuart Murdock and Schrödinger Inc. for the scientific and technical partnership and to the Chemical Computing Group for the long and fruitful collaboration.

Supporting Information Available: Information concerning starting poses, net charges, and keto-enol and tautomeric forms used for each molecule. This material is available free of charge via the Internet at <http://pubs.acs.org>.

REFERENCES AND NOTES

- (1) Cohen, P. The origins of protein phosphorylation. *Nat. Cell Biol.* **2002**, *4*, E127–E130.
- (2) Manning, G.; Whyte, D. B.; Martinez, R.; Hunter, T.; Sudarsanam, S. The protein kinase complement of human genome. *Science* **2002**, *298*, 1912–1934.
- (3) Blume-Jensen, P.; Hunter, T. Oncogenic kinase signaling. *Nature* **2001**, *411*, 355–365.
- (4) Cohen, P. Protein kinases- the major drug targets of the twenty-first century? *Nat. Rev.* **2002**, *1*, 309–315.
- (5) Pinna, L. A. A historical view of protein kinase CK2. *Cell. Mol. Biol. Res.* **1994**, *40*, 383–390.
- (6) Meggio, F.; Pinna, L. A. One-thousand-and-one substrates of protein kinase CK2? *FASEB J.* **2003**, *17*, 349–368.
- (7) Canton, D. A.; Litchfield, D. W. The shape of things to come: an emerging role for protein kinase CK2 in the regulation of cell morphology and the cytoskeleton. *Cell Signalling* **2006**, *18*, 267–275.
- (8) Tawfic, S.; Yu, S.; Wang, H.; Faust, R.; Davis, A.; Ahmed, K. Protein kinase CK2 signal in neoplasia. *Histol. Histopathol.* **2001**, *16*, 573–582.
- (9) Guerra, B.; Issinger, O.-G. Protein kinase CK2 and its role in cellular proliferation, development and pathology. *Electrophoresis* **1999**, *20*, 391–408.
- (10) Pinna, L. A.; Meggio, F. Protein kinase CK2 (“casein kinase-2”) and its implication in cell division and proliferation. *Prog. Cell Cycle Res.* **1997**, *3*, 77–97.
- (11) Molier, D. E.; Moro, S.; Sarno, S.; Zagotto, G.; Zanotti, G.; Pinna, L. A.; Battistutta, R. Inhibition of protein kinase CK2 by anthraquinone-related compounds. A structural insight. *J. Biol. Chem.* **2003**, *278*, 1831–1836.
- (12) Battistutta, R.; Sarno, S.; De Molier, E.; Papinutto, E.; Zanotti, G.; Pinna, L. A. The replacement of ATP by the competitive inhibitor emodin induces conformational modifications in the catalytic site of protein CK2. *J. Biol. Chem.* **2000**, *275*, 29618–29622.
- (13) Sarno, S.; De Molier, E.; Ruzzene, M.; Pagano, M. A.; Battistutta, R.; Bain, J.; Fabbro, D.; Schoepfer, J.; Elliott, M.; Furet, P.; Meggio, F.; Zanotti, G.; Pinna, L. A. Biochemical and three-dimensional-structural study of the specific inhibition of protein kinase CK2 by [5-oxo-5,6-dihydroindolo-(1,2-a)quinazolin-7-yl]acetic acid (IQA). *Biochem. J.* **2003**, *374*, 639–646.
- (14) Battistutta, R.; De molier, E.; Sarno, S.; Zanotti, G.; Pinna, L. A. Structural features underlying selective inhibition of protein kinase CK2 by ATP site-directed tetrabromo-2-benzotriazole. *Protein Sci.* **2001**, *10*, 2200–2206.
- (15) Meggio, F.; Shugar, D.; Pinna, L. A. Ribofuranosyl-benzimidazole derivatives as inhibitors of casein kinase-2 and casein kinase-1. *Eur. J. Biochem.* **1990**, *187*, 89–94.
- (16) Sarno, S.; Moro, S.; Meggio, F.; Zagotto, G.; Dal Ben, D.; Ghisellini, P.; Battistutta, R.; Zanotti, G.; Pinna, L. A. Toward the rational design of protein kinase casein kinase-2 inhibitors. *Pharmacol. Ther.* **2002**, *93*, 159–168.
- (17) Agullo, G.; Gamet-Payrastra, L.; Manenti, S.; Viala, C.; Remesy, C.; Chap, H.; Payrastra, B. Relationship between flavonoid structure and inhibition of phosphatidylinositol 3-kinase: a comparison with tyrosine kinase and protein kinase C inhibition. *Biochem. Pharmacol.* **1997**, *53*, 1649–1657.
- (18) Meggio, F.; Pagano, M. A.; Moro, S.; Zagotto, G.; Ruzzene, M.; Sarno, S.; Cozza, G.; Bain, J.; Elliott, M.; Deana, A. D.; -Brunati, A. M.; Pinna, L. A. Inhibition of protein kinase CK2 by condensed polyphenolic derivatives. An in vitro and in vivo study. *Biochemistry* **2004**, *43*, 12931–12936.
- (19) Pagano, M. A.; Andrzejewska, M.; Ruzzene, M.; Sarno, S.; Cesaro, L.; Bain, J.; Elliott, M.; Meggio, F.; Kazimierczuk, Z.; Pinna, L. A. Optimization of protein kinase CK2 inhibitors derived from 4,5,6,7-tetrabromobenzimidazole. *J. Med. Chem.* **2004**, *47*, 6239–6247.
- (20) Andrzejewska, M.; Pagano, M. A.; Meggio, F.; -Brunati, A. M.; Kazimierczuk, Z. Polyhalogenobenzimidazoles: synthesis and their inhibitory activity against casein kinases. *Bioorg. Med. Chem.* **2003**, *11*, 3997–4002.
- (21) Pagano, M. A.; Meggio, F.; Ruzzene, M.; Andrzejewska, M.; Kazimierczuk, Z.; Pinna, L. A. 2-Dimethylamino-4,5,6,7-tetrabromo-1H-benzimidazole: a novel powerful and selective inhibitor of protein kinase CK2. *Biochem. Biophys. Res. Commun.* **2004**, *321*, 1040–1044.
- (22) Battistutta, R.; Mazzorana, M.; Sarno, S.; Kazimierczuk, Z.; Zanotti, G.; Pinna, L. A. Inspecting the structure-activity relationship of protein kinase CK2 inhibitors derived from tetrabromo-benzimidazole. *Chem. Biol.* **2005**, *12*, 1211–1219.
- (23) Åquist, J.; Medina, C.; Samuelsson, J.-E. A new method for predicting binding affinity in computer-aided drug design. *Protein Eng.* **1994**, *7*, 385–391.
- (24) Hansson, T.; Åquist, J. Estimation of binding-free energies for HIV proteinase inhibitors by molecular dynamics simulation. *Protein Eng.* **1995**, *8*, 1137–1144.
- (25) -Brandsdal, B. O.; Aqvist, J.; Smalas, A. O. Computational analysis of binding of P1 variants to trypsin. *Protein Sci.* **2001**, *10*, 1584–1595.
- (26) Chen, J.; Wang, R.; Taussig, M.; Houk, K. N. Quantitative calculations of antibody-antigen binding: steroid-DB3 binding energies by the linear interaction energy method. *J. Org. Chem.* **2001**, *66*, 3021–3026.
- (27) Dey, I. Exploring the interaction of some N-benzoyloxycarbonyl-L-phenyl alanyl-L-alanine ketones and bovine spleen cathepsin B by molecular modeling and binding free energy calculation. *J. Biomol. Struct. Dyn.* **1999**, *16*, 891–900.
- (28) Graffner-Nordberg, M.; Kolmodin, K.; Aqvist, J.; Queener, S. F.; Hallberg, A. Design, synthesis, computational prediction, and biological evaluation of ester soft drugs as inhibitors of Dihydrofolate Reductase from *Pneumocystis carinii*. *J. Med. Chem.* **2001**, *44*, 2391–2402.

- (29) Hou, T. J.; Zhang, W.; Xu, X. J. Binding affinities for a series of selective inhibitors of Gelatinase-A using molecular dynamics with a linear interaction energy approach. *J. Phys. Chem. B* **2001**, *105*, 5304–5315.
- (30) Hou, T.-J.; Zhang, W.; Xu, X.-J. Binding free energy calculations for MMP2-hydroxamate complexes. *Huaxue Xuebao* **2002**, *60*, 221–227.
- (31) Lamb, M. L.; Tirado-Rives, J.; Jorgensen, W. L. estimation of the binding affinities of FKBP12 inhibitors using a linear response method. *Bioorg. Med. Chem.* **1999**, *7*, 851–860.
- (32) Luzhkov, V. B.; Aqvist, J. Mechanisms of tetraethylammonium ion block in the KcsA potassium channel. *FEBS Lett.* **2001**, *495*, 191–196.
- (33) Marelius, J.; Graffner-Nordberg, M.; Hansson, T.; Hallberg, A.; Aqvist, J. Computation of affinity and selectivity: binding of 2,4-diaminopteridine and 2,4-diaminoquinazoline inhibitors to dihydrofolate reductases. *J. Comput.-Aided Mol. Des.* **1998**, *12*, 119–131.
- (34) Sham, Y. Y.; Chu, Z. T.; Tao, H.; Warshel, A. Examining methods for calculations of binding free energies: LRA, LIE, PDL-D-LRA, and PDL-D-S-LRA calculations of ligands binding to an HIV protease. *Proteins: Struct., Funct., Genet.* **2000**, *39*, 393–407.
- (35) Smith, R. H., Jr.; Jorgensen, W. L.; Tirado-Rives, J.; Lamb, M. L.; Janssen, P. A. J.; Michejda, C. J.; Smith, M. B. K. Prediction of binding affinities for TIBO inhibitors of HIV-1 reverse transcriptase using Monte Carlo simulations in a linear response method. *J. Med. Chem.* **1998**, *41*, 5272–5286.
- (36) Wang, W.; Wang, J.; Kollman, P. A. What determines the van der Waals coefficient β in the LIE (Linear Interaction Energy) method to estimate binding free energies using molecular dynamics simulations? *Proteins: Struct., Funct., Genet.* **1999**, *34*, 395–402.
- (37) Wesolowski, S. S.; Jorgensen, W. L. Estimation of binding affinities for Celecoxib analogues with COX-2 via Monte Carlo-extended linear response. *Bioorg. Med. Chem. Lett.* **2002**, *12*, 267–270.
- (38) Huang D.; Caflisch, A. Efficient evaluation of binding free energy using continuum electrostatics solvation. *Med. Chem.* **2004**, *47*, 5791–5797.
- (39) Jones-Hertzog, D. K.; Jorgensen, W. L. Binding affinities for sulfonamide inhibitors with human thrombin using Monte Carlo simulations with a linear response method. *J. Med. Chem.* **1997**, *40*, 1539–1549.
- (40) Ljungberg, K. B.; Marelius, J.; Musil, D.; Svensson, P.; Norden, B.; Aqvist, J. Computational modelling of inhibitor binding to human thrombin. *Eur. J. Pharm. Sci.* **2001**, *12*, 441–446.
- (41) Wang, J.; Dixon, R.; Kollman, P. A. Ranking ligand binding affinities with Avidin: a molecular dynamics-based interaction energy study. *Proteins: Struct., Funct., Genet.* **1999**, *34*, 69–81.
- (42) Lill, M. A.; Winiger, F.; Vedani, A.; Ernst, B. Impact of induced fit on ligand binding to the androgen receptor: a multidimensional QSAR study to predict endocrine-disrupting effects of environmental chemicals. *J. Med. Chem.* **2005**, *48*, 5666–5674.
- (43) Osterberg, F.; Aqvist, J. Exploring blocker binding to a homology model of the open hERG K⁺ channel using docking and molecular dynamics methods. *FEBS Lett.* **2005**, *579*, 2939–2944.
- (44) Zhou, R.; Friesner, R. A.; Ghosh, A.; Rizzo, R. C.; Jorgensen, W. J.; et al. New linear interaction method for binding affinity calculations using a continuum solvent model. *J. Phys. Chem. B* **2001**, *102*, 10388–10397.
- (45) Tounge, B. A.; Reynolds, C. H. Calculation of the binding affinity of β -secretase inhibitors using the linear interaction energy method. *J. Med. Chem.* **2003**, *46*, 2074–2082.
- (46) Singh, P.; Mhaka, A. M.; Christensen, S. B.; Gray, J. J.; Denmeade, S. R.; Isaacs, J. T. Applying linear interaction energy method for rational design of noncompetitive allosteric inhibitors of the sarco- and endoplasmic reticulum calcium-ATPase. *J. Med. Chem.* **2005**, *48*, 3005–3014.
- (47) Carlson, A.; Jorgensen, W. L. An extended linear response method for determining free energies of hydration heather. *J. Phys. Chem.* **1995**, *99*, 10667–10673.
- (48) Gallicchio, E.; Zhang, L. Y.; Levy, R. M. The SGB/NP hydration free energy model based on the surface generalized born solvent reaction field and novel nonpolar hydration free energy estimators. *J. Comput. Chem.* **2002**, *23*, 517–529.
- (49) Berman, H. M.; Westbrook, J.; Feng, Z.; Gilliland, G.; Bhat, T. N.; Weissig, H.; Shindyalov, I. N.; Bourne, P. E. The protein data bank. *Nucleic Acids Res.* **2000**, *28*, 235–242.
- (50) Niefind, K.; Guerra, B.; Ermakowa, I.; Issinger, O. G. Crystal structure of human protein kinase Ck2: insights into basic properties of the Ck2 holoenzyme. *EMBO J.* **2001**, *20*, 5320–5331.
- (51) *Liaison*, version 3.5; Schrödinger, LLC: New York, NY, 2005.
- (52) *LigPrep*, version 1.6; Schrödinger, LLC: New York, NY, 2005.
- (53) *Molecular Operating Environment (MOE 2005.06)*; Chemical Computing Group, Inc.: 1255 University Street, Suite 1600, Montreal, Quebec, Canada H3B 3X3, 2005.
- (54) *Spartan'02*; Wavefunction, Inc.: Irvine, CA.
- (55) Chambers, C. C.; Hawkins, G. D.; Cramer, C. J.; Truhlar, D. G. Model for aqueous solvation based on class IV atomic charges and first solvation shell effects. *J. Phys. Chem.* **1996**, *100*, 16385–16398.
- (56) Pospisil, P.; Kuoni, T.; Scapozza, L.; Folkers, G. Methodology and problems of protein-ligand docking: case study of dihydroorotate dehydrogenase, thymidine kinase, and phosphodiesterase 4. *J. Recept. Signal Transduction Res.* **2002**, *22*, 141–154.
- (57) Cozza, G.; Bovini, P.; Zorzi, E.; Paletto, G.; Pagano, M. A.; Sarno, S.; Donella-Deana, A.; Zagotto, G.; Rosolen, A.; Pinna, L. A.; Meggio, F.; Moro, S. Identification of ellagic acid as potent inhibitor of protein kinase CK2: a successful example of a virtual screening application. *J. Med. Chem.* **2006**, *49*, 2363–2366.

CI600369N